Eur. Phys. J. D **44**, 57–63 (2007)
DOI: 10.1140/epjd/e2007-00184-7

THE EUROPEAN PHYSICAL JOURNAL D

Photofragment space distribution in the photodissociation of NaI in the spectral range 315–370 nm: the role of molecular axis rotation

K.O. Korovin[1], E. Heinecke[2], A. Patzer[1], T. Liebig[2], O.S. Vasyutinskii[1,a], and D. Zimmermann[2]

[1] Ioffe Physico-Technical Institute, Russian Academy of Sciences, 194021 Saint-Petersburg, Russia
[2] Institute of Atomic Physics, Technical University of Berlin, 10623 Berlin, Germany

Received 12 December 2006 / Received in final form 22 March 2007
Published online 6 June 2007 –

Abstract. The first determination of translational anisotropy parameters β in the photodissociation of NaI molecules in the spectral range 315–370 nm is reported. The anisotropy parameters were determined by the analysis of Doppler resolved absorption profiles of Na($^2S_{1/2}$) atoms produced in the photodissociation of NaI by linearly polarized light. The profiles were recorded for two orientations of the photolysis light: parallel and perpendicular to the direction of the probe beam. The value of the parameter β was obtained from a simultaneous fit of the profiles. The role of the rotation of the parent molecules on the branching ratio between parallel and perpendicular transitions in NaI during dissociation is discussed.

PACS. 33.80.-b Photon interactions with molecules – 33.80.Be Level crossing and optical pumping – 33.80.Gj Diffuse spectra; predissociation, photodissociation

Introduction

The dynamics of molecular photodissociation can efficiently be studied by the analysis of the vector properties of recoiling photofragments, see for instance the review papers [1,2]. Such vector properties as the fragment angular momentum **j** polarization (orientation and alignment) and the anisotropy of the fragment recoil velocity **v** with respect to the laboratory axis **Z** are usually classified as $\mathbf{j}-\mathbf{Z}$ and $\mathbf{v}-\mathbf{Z}$ correlation, respectively [1–3]. However, the most detailed information about the photodissociation dynamics can be obtained by the analysis of the correlation between the fragment angular momentum polarization j and the recoil velocity **v** [1,2]. The full quantum mechanical treatment of the correlation between the spatial anisotropy and the angular momentum polarization of the fragments has been given in the axial recoil approximation by Siebbeles et al. [4]. The effect of rotation of the recoil axis on the angular momentum polarization of the fragments has recently been treated quantum mechanically by Kuznetsov and Vasyutinskii [5]. The experimental determination of the angular momentum **j** polarization of the fragments can provide the most detailed information about the dissociation dynamics: the symmetry of the molecular states involved in the photoprocess, possible coherent effects, non-adiabatic interactions between the molecular states, etc. [4,5].

The angular momentum photofragment space distribution can in general be presented as an expansion over the angular dependent state multipoles ρ_{KQ} [3] of rank $K = 0...2j$ and projection $Q = -K...K$ which in the case of photodissociation are functions of the recoil angles θ and ϕ [6]. The recoil-angle-independent quantities which contain all dynamical information and are usually determined from experiment are the anisotropy parameters of rank K. The anisotropy parameters can be expressed either in the laboratory frame [7], or in the molecule-fixed body frame [8]. In both cases the zero-rank anisotropy parameter is equivalent to the well-known parameter β which describes the spatial distribution of the photofragments after photodissociation [3].

In the present paper we report the first experimental determination of the parameter β in NaI photodissociation at different wavelength in the spectral range 315–370 nm.

The alkali halides represent a classical example of molecules where the photodissociation occurs simultaneously via several excited molecular states. For almost all alkali-halides the bound molecular ground state is ionic and shows an avoided crossing with the lowest excited state at large internuclear separation [9,10]. The five lowest electronic excited states are covalent and form the first manifold which corresponds to the dissociation limit where the alkali and halogene atom are in their ground states $^2S_{1/2}$ and $^2P_{3/2}$, respectively. The potential curves of these five states are close to each other which can cause non-adiabatic interaction between the states of the same

[a] e-mail: asv@pms.ioffe.ru

symmetry which is known to play an important role in the photodissociation dynamics. Similar considerations apply to the next higher group of excited molecular electronic states (the second manifold), where three electronic states approach the same dissociation limit corresponding to the ground state alkali atom and the halogene atom in the metastable $^2P_{1/2}$ state [10].

The structure and photodissociation dynamics of the alkali halides have been studied for decades both experimentally and theoretically [9–19]. However, the subject is still far from being well understood. Su and Riley [11] and Anderson et al. [12] investigated the angular distribution of the alkali photofragments in molecular beam experiments using time-of-flight methods and determined dissociation energies and the parallel/perpendicular characters of the dissociation transitions for the whole set of the alkali iodide molecules at 266 and 347.1 nm. The experimental values of the parameter β in NaI reported by Su and Riley [11] at 266 nm and by Anderson et al. [12] at 347.1 nm are $\beta = 0.7 \pm 0.08$ and $\beta = -0.64 \pm 0.18$, respectively[1].

Korovin et al. [13–15] have recently investigated the dynamics of RbI photodissociation at 266 nm using sub-Doppler spectroscopy of spin-polarized rubidium $5^2S_{1/2}$ photofragments and determined the complete set of anisotropy parameters describing coherent and non-coherent excitation as well as non-adiabatic dynamics in the reaction channel resulting in the spin-orbit excited iodine atoms. An important result of this study is the experimental determination of the phases and amplitudes of the photodissociation T-matrix [15].

NaI is a benchmark system for the study of a nonadiabatic interaction phenomenon in the vicinity of a level-crossing area. The level crossing problem in NaI has attracted much attention both in early works [9–12] and in recent study utilizing real-time pump-and-probe technique. The level crossing problem has been investigated by Zewail et al. [16,17] using the femtosecond transition state spectroscopy. Zewail and co-workers reported the observation of the recurrences of a persistent wave packet over a long time period and studied the dynamics by the crossing area between the covalent $A0^+$ and the ionic ground state $X0^+$potential energy curves.

An ab initio configuration interaction computation of the photodissociation dynamics in NaI has recently been performed by Alekseyev et al. [18] yielding all low-lying potential energy curves, spin-orbit coupling matrix elements and transition dipole moments. These results were used to construct diabatic and adiabatic representations of the molecular states being relevant for the femtosecond studies and showed good agreement with the experimental data of Zewail and co-workers.

The discrete features between 300 nm and 370 nm were studied by Schäfer et al. [19] using high resolution laser spectroscopy and were assigned to rovibronic transitions between the $X0^+$ and the predissociative $A0^+$ state. The range from 245 nm and 256 nm was analyzed by Bluhm et al. [20] and assigned to discrete transitions between the $X0^+$ and the predissociative $C0^+$ state. Baba et al. [21] have presented the detailed analysis of the shape of the experimentally resolved rotational lines in the $X0^+ \rightarrow A0^+$ transition.

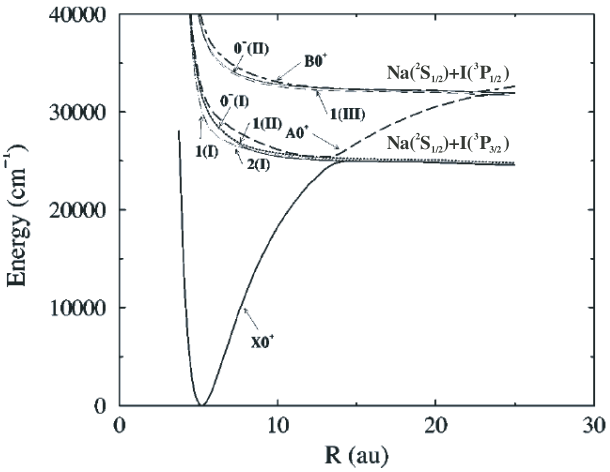

Fig. 1. Ab initio potential curves for several lowest electronic states of NaI [18]. The final states of the fragments are added to the plot.

In spite of all these achievements, only very coarse experimental information exists until now on the structure and dynamics of the four repulsive states of the first manifold and the two repulsive states of the second manifold in NaI. The aim of the present work is to obtain the most possible detailed information about the photodissociation dynamics in NaI via the first and the second excited state manifolds analyzing the angular momentum photofragment distribution by means of the Doppler polarization spectroscopy. This first paper presents the determination and analysis of the parameter β as function of the photolysis photon energy in the spectral range 315–370 nm, while the determination and analysis of other anisotropy parameters will follow in a future paper.

1 Theoretical background and experimental method

Sodium iodide possesses an ionic $X^1\Sigma_0^+$ ground state and several excited states which can dissociate into neutral or ionic fragments [10]. The ab initio potential energy curves of the ground and lowest excited states of NaI from reference [18] are shown in Figure 1. Due to the strong spin-orbit interaction, Hund's coupling case c [22] is appropriate to label the electronic states, i.e. only the projection $\boldsymbol{\Omega}$ of the total angular momentum $\mathbf{J}$ onto the molecular axis $\mathbf{Z}'$ is a good quantum number and the excited electronic states which belong to the first manifold are labeled by the $\boldsymbol{\Omega}$ value: $A0^+$, 0^-(I), 1(I), 1(II), and 2(I), as shown in Figure 1. Three of these states: $A0^+$, 1(I), and 1(II) can be optically excited from the ground state with respect to the selection rules for dipole transitions [22]. The

[1] Note, that the factor b experimentally determined in references [11,12] is expressed in terms of the parameter β used in this paper as $\beta = 2b$.

optical transition $X^1\Sigma_0^+ \rightarrow A0^+$ is of parallel character, while the transitions $X^1\Sigma_0^+ \rightarrow 1(I)$, $1(II)$ are of perpendicular character. The absorption spectrum of NaI in the wavelength region from 200 to 400 nm at the temperature range of 1000–1100 K was first observed by Davidovits and Broadhead [9] almost 50 years ago and since that time was reproduced several times by other authors. Davidovits and Broadhead [9] reported a continuum absorption spectrum with three broad maxima which they assigned to the photodissociation via three different low-lying electronic energy states resulting in the following dissociation channels:

$$\mathrm{NaI}(^1\Sigma_0^+) + h\nu_1(220\ \mathrm{nm}) \rightarrow \mathrm{Na}(3^2\mathrm{P}_{1/2,3/2}) + I(5^2\mathrm{P}_{3/2}), \quad (1)$$

$$\mathrm{NaI}(^1\Sigma_0^+) + h\nu_2(255\ \mathrm{nm}) \rightarrow \mathrm{Na}(3^2\mathrm{S}_{1/2}) + I(5^2\mathrm{P}_{1/2}), \quad (2)$$

$$\mathrm{NaI}(^1\Sigma_0^+) + h\nu_3(325\ \mathrm{nm}) \rightarrow \mathrm{Na}(3^2\mathrm{S}_{1/2}) + I(5^2\mathrm{P}_{3/2}). \quad (3)$$

In their recent paper Alekseyev and co-workers [18] have computed the corresponding potential energy curves taking into account strong spin orbit coupling. These results reveal an avoided crossing between the $X0^+$ and the $A0^+$state creating a bounding minimum.

The details of our experimental method were outlined elsewhere [13–15]. Briefly, linearly polarized photolysis light at 315–370 nm from a frequency doubled pulsed dye laser initiated the photodissociation reaction according to equation (3) which results in the ground state sodium and iodine atomic photofragments. Unlike our previous experiments [13–15] which were carried out under bulk conditions, an effusive molecular beam of parent NaI molecules was used in the current experiment. For linearly polarized photolysis light, when the laboratory Z-axis is parallel to the polarization vector $\mathbf{e}$, the angular distribution of the photofragment recoil is given by the well-known formula [3]:

$$W(\theta) = \frac{1}{4\pi}[1 + \beta P_2(\cos\theta)], \quad (4)$$

where β is the zero-rank anisotropy parameter, θ is the recoil polar angle, and $P_2(\cos\theta)$ is the Legendre polynomial of second order.

The shape of the Doppler absorption profile of the sodium fragments on the transition $3^2\mathrm{S}_{1/2} \rightarrow 3^2\mathrm{P}_{1/2}$ at 589.756 nm was monitored by a tunable narrow-band continuous wave probe laser propagating either parallel or perpendicular to the photolysis light polarization vector.

In general case, the absorption Doppler profile can be written as [14]:

$$\Delta I_\vartheta(\Delta\omega) = A_t \int_{\frac{|\Delta\omega|}{k}}^{\infty} \left[1 + \beta P_2(\cos\vartheta) P_2\left(\frac{\Delta\omega}{kv}\right)\right] f(v) v\, dv \quad (5)$$

where $\Delta\omega = \omega - \omega_0$ is the frequency detuning of the probe laser from the center of the atomic absorption line, k is the modulus of the wave vector of the probe light, v is the modulus of the fragment relative velocity, A_t is a constant, ϑ is the angle between the direction of probe light propagation and the photolysis light polarization vector $\mathbf{e}$ (Z-axis), and $f(v)$ is the fragment velocity distribution, which in case of a diatomic molecule is associated with the velocity distribution of the parent molecules and can be approximated with a Gaussian function:

$$f(v) = \frac{1}{v_0^2 + s_0^2} \frac{1}{\sqrt{2\pi s_0^2}} \exp\left[-\frac{(v - v_0)^2}{2s_0^2}\right], \quad (6)$$

where v_0 is the mean fragment recoil velocity and s_0 is the mean thermal velocity of the parent molecules corresponding to the oven temperature.

Equation (5) was derived assuming that the Doppler broadened atomic fragment absorption line is much larger than the natural atomic linewidth, which is obviously true in our experimental conditions.

As seen from equation (5), the difference between the absorption profiles $I_0 - I_{\pi/2}$ does not contain the isotropic part and is directly proportional to the parameter β. This difference together with the profiles I_0 and $I_{\pi/2}$ were used in this work for determination of the parameter β from experiment.

In the condition of our experiment the mean thermal velocity of the parent molecules in equation (6) was about $s_0 \approx 500$ m/s and the mean recoil velocity of the fragments was about $v_0 \approx 1500$–2000 m/s depending on the photolysis wavelength. The corresponding Doppler width of the atomic absorption profiles was about 4–6 GHz, see Figure 3, which resulted in a partial overlap of the four hyperfine structure (hfs) components $F_e = 1, 2 \leftarrow F_g = 1, 2$ in the probe transition $3^2\mathrm{P}_{1/2} \leftarrow 3^2\mathrm{S}_{1/2}$ (see Fig. 3). The hfs structure of the probe line was treated in our fitting procedure using all four hfs structure lines fixed at the frequencies of: -0.782, -0.593, 0.989, and 1.178 GHz, with the relative intensities of: 1, 1, 0.2, and 1, respectively. The intensity ratio was obtained through the summation of the statistical weights of the hyperfine transitions for $\Delta m = 0$ and fits well to the experimental data. No population redistribution by other processes, e.g. dissociation dynamics occurs. No significant difference to the values of the β parameter obtained by a simpler fitting procedure neglecting the upper state hfs splitting of 189 MHz was found.

2 Experimental

The schematic view of our experimental set-up is shown in Figure 2. The linearly polarized UV photolysis laser beam crossed the effusive molecular beam at the angle of 90°, several millimeters away from the nozzle and dissociated a small fraction of NaI molecules. Ground state sodium atoms produced by the pulse drifted out of the probe beam volume causing a transient absorption of probe light of a few μs time scale. The Doppler absorption profiles of the produced sodium atoms were monitored by tuning the frequency of the probe cw-ring laser over the sodium $3^2\mathrm{S}_{1/2} \rightarrow 3^2\mathrm{P}_{1/2}$ resonance D_1 line at 589.756 nm.

The effusive molecular beam was produced by an electrically-heated oven with a nozzle of 1 mm diameter and a NaI salt compartment of about 20 mm length.

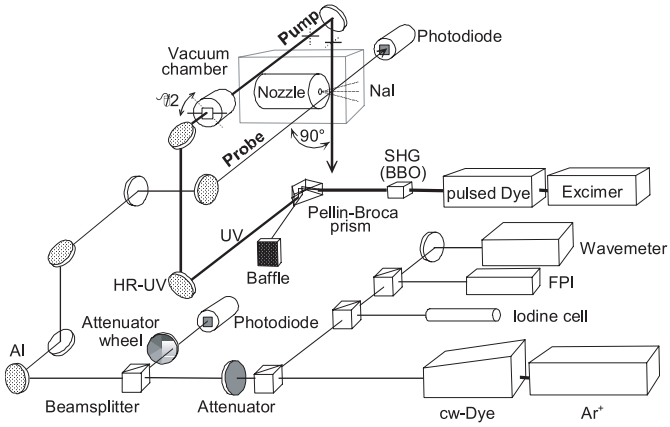

Fig. 2. Schematic diagram of the experimental set-up.

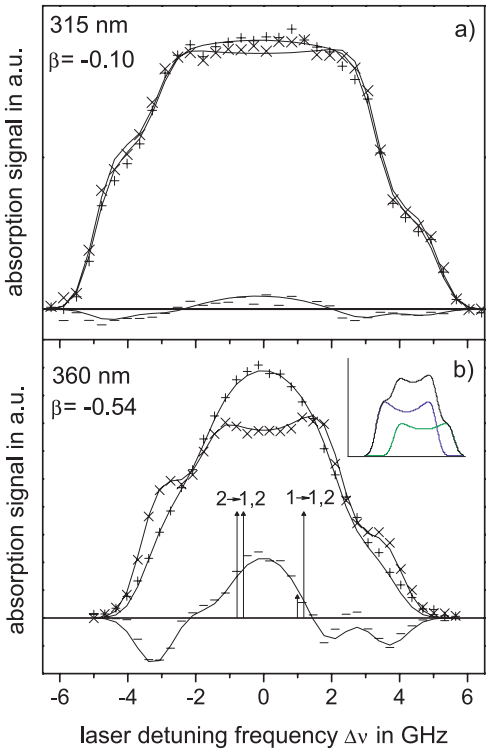

Fig. 3. Typical experimental Doppler profiles at 315 nm (a) and 360 nm (b) of the pump light for different polarization geometries: (+) polarization of the pump light is parallel to the probe light beam (×) polarization of the pump light is perpendicular to the probe light beam (−) difference between (+) and (−). The solid line is the result of simultaneous fit of the plots according to equation (5). The arrows indicate the frequencies and relative intensities of the two pairs of unresolved hyperfine structure lines. The insert in (b) clarifies how the "perpendicular" Doppler profile arises from the sum of two hfs lines.

The measurements were performed at oven temperatures of about 580–600 °C which provided sufficient density of the molecules in the beam and avoided thermal dissociation. The oven was placed into a vacuum chamber with fused silica windows which was evacuated down to 10^{-6} mbar residual gas pressure.

The photolysis light was the output of a frequency doubled excimer pumped dye laser (Lambda Physics, FL 2002) which was tuned in 5 and 1 nm steps over the spectral range of 315–370 nm using several different dyes from Rhodamine 6G to Pyridine I. The photolysis laser wavelength selection was performed using the forth or fifth order reflection from a 600 lines/mm grating, resulting in a line bandwidth in the UV of about 0.4 cm^{-1}. The 180 mJ output of the XeCl excimer laser (Lambda Physics, LPX 205i) operated at 8 Hz repetition rate in a continuous mode resulted in 8...15 mJ per pulse of the dye laser, depending on the wavelength. After frequency doubling of the dye laser output with a BBO crystal, the second harmonic was separated from the fundamental by means of a Pellin-Broca prism and finally resulted in typical UV pulse energies of about 0.75...2.25 mJ. Two sets of HR-UV mirrors from 300 nm to 350 nm (Edmund) and 350 nm to 370 nm (Thorlabs) were used to bring the UV photolysis light into the chamber by a fused silica window on top. The direction of the photolysis laser polarization vector was controlled by means of a UV $-\lambda/2$ Fresnel rhomb (Gsänger) driven by a PC-controlled step-motor.

The probe laser system consisted of a continuous wave Ar^+ laser (Coherent, Innova 200) which served as a pump of a ring-dye laser (Coherent, CR699-21) using the dye Rhodamine 6G. The dye laser beam with a power of several hundred mW was split several times to provide input signals to a confocal Fabry-Perot interferometer (FPI) with a free spectral range of 300 MHz, an iodine absorption cell, and a wavemeter (Burleigh, WA20) which were used for the relative and absolute frequency and mode structure control. The probe laser linewidth was about 1 MHz which was much smaller than the photofragment Doppler absorption profile. The main probe laser beam was then attenuated down to 50 mW and splitted into two beams of about 25 mW each, which were used as the probe and the reference beams. The probe beam was guided by Al-coated mirrors and passed by a fused silica window into the chamber. The intensities of the probe and the reference beams were detected by two fast photodiodes (Thorlabs, PDA 155) and then monitored by a digital oscilloscope (Tektronix, TDS 320 or TDS2012). An attenuation wheel in front of the reference photodiode was used to equalize the reference and probe signal DC baselines at typically 300 mV level. The measurements were carried out with the scope's probe channel switched to AC mode to get optimized digital resolution of the small absorption signals with typical amplitude of about 15 mV. The probe laser was scanned over the sodium D_1 line by a 12...15 GHz range in 3...5 MHz steps. At an appropriate number of equidistant frequency points the signals from the photodiodes were accumulated for both pump laser polarization directions using the scope averaging over 128 or 256 pump pulses. The complete set-up including lasers and oscilloscope was ruled by a computer using a special program written in LabView.

A typical probe laser scan contained 30–38 exponentially decaying absorption signals, corresponding to

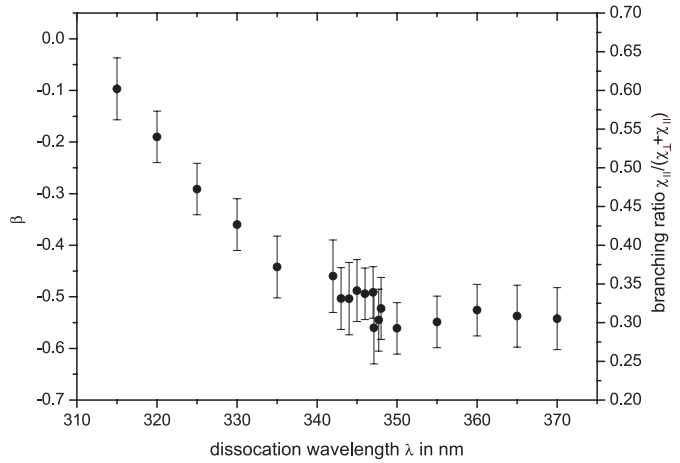

Fig. 4. Experimental values of the parameter β versus the photolysis laser wavelength λ. The right axis shows the branching ratio according to equation (8).

different detunings of the probe laser frequency from the center of the sodium absorption line. Each signal was normalized by the corresponding reference signal and then fitted with an exponential function for determining the absorption amplitude at the time of the pump laser shot. The frequency axis for Doppler profiles was calculated by linear interpolation of the transmission peaks from FPI signal. Zero detuning corresponds to the transition energy of 16956.145 cm^{-1} of the sodium $3^2S_{1/2} \rightarrow 3^2P_{1/2}$transition without taking hyperfine splitting into account. The value of β was obtained by simultaneous fitting of Doppler profiles according to equation (5). A typical probe laser scan with the fit is shown in Figure 3. The complicated shape of the Doppler profiles in Figures 3a, 3b is a result of summation of two unresolved hfs Doppler lines as clarified in the insert in the upper right corner of Figure 3b, where each line corresponds to a certain ground state hfs sublevel. The hfs lines are single-peaked if the fragments move mainly perpendicular to the probe beam and double-peaked if the fragments move mainly parallel to the probe beam. For each photolysis laser wavelength the measurements were repeated three, or more times. The resulting standard deviations of the β parameters plus an additional error of 0.04 accounting for angular and depolarization uncertainties are given as error bars in Figure 4.

3 Results and discussion

All measured Doppler profiles can well be fitted by the function presented in equation (5). The determined values of the parameter β are presented in Figure 4 as function of the photolysis light wavelength. All these values are negative and show a steep decrease from the largest value of $\beta \approx -0.10$ at 315 nm to $\beta = -0.56 \pm 0.08$ at 347.1 nm and then a plateau up to 370 nm. Our value of the parameter $\beta = -0.56 \pm 0.08$ at 347.1 nm is in an excellent agreement with the value $\beta = -0.64 \pm 0.18$ reported by Anderson et al. [12] within the experimental error bars.

The obtained values of the parameter β contain the information on the branching ratios of the parallel/perpendicular transition intensities in NaI as well as on the molecular axis rotation during dissociation. However, the determination of this information from experimental data is not a trivial procedure because the *perpendicular* transitions in NaI in the spectral region 300–370 nm occur via the *unbound continuum energy states* 1(I) and 1(II), while the *parallel* transition occurs via the predissociative *quasibound discrete energy state* $A0^+$, as shown in Figure 1.

The perpendicular transitions to the two $\Omega = 1$ continua can be described by equation (4) where the parameter β is equal to $\beta_\perp = -P_2(\cos\gamma)$ [23] and γ is the classical angle of rotation of the molecular axis during dissociation. According to reference [12], the angle γ in NaI is relatively small, $\gamma = 13^\circ$ and therefore the Legendre polynomial $P_2(\cos\gamma)$ can be put equal to unity, resulting in $\beta_\perp = -1$. The parallel transition to the quasibound $\Omega = 0^+$ state can also be described by the same equation (4), where the corresponding parameter $\beta_{||}$ differs from the usual value $\beta_{||} = 2$ [3], because the molecule undergoes many periods of rotation before the dissociation occurs. In case of excitation of an isolated predissociative rotational state, the residual fragment angular distribution depends on the rotational branch (P, R, or Q) in the optical transition. In the high-J limit which meets the condition of our experiment, the P and R branches lead to the same value of β, $\beta = 1/2$, while the Q branch leads to $\beta = -1$ [24]. As no Q branch exists in the parallel $X^1\Sigma_0^+ \rightarrow A0^+$ transition [22], the residual β value is equal to $\beta_{||} = 1/2$ in this case. In general, if both parallel and perpendicular excitations occur, the exact quantum mechanical approach gives the angular distribution in equation (4) with the following parameter β [25]:

$$\beta = \frac{f_0(0,0) - 4f_0(1,1)P_2(\cos\gamma)}{2[f_0(0,0) + 2f_0(1,1)]}, \qquad (7)$$

where $f_0(0,0)$ and $f_0(1,1)$ are zero-rank dynamical functions [6,25] describing the parallel and perpendicular dissociative transitions, respectively.

The expression for the parameter β in equation (7) describes the photodissociation of NaI in the short-lifetime limit in the 1(I) and 1(II) channels and the long-lifetime limit in the $A0^+$ channel. It is equivalent to the model used by Anderson et al. [12]. The relative intensity of the parallel excitation which follows from equation (7) in case $P_2(\cos\gamma) \approx 1$ is:

$$\frac{\chi_{||}}{\chi_\perp + \chi_{||}} = \frac{f_0(0,0)}{2f_0(1,1) + f_0(0,0)} = \frac{2}{3}(\beta + 1), \qquad (8)$$

where the terms $\chi_{||} = f_0(0,\,0)$ and $\chi_\perp = 2\ f_0(1,\,1)$ are proportional to the intensities of the parallel and perpendicular transitions, respectively.

The branching ratio in equation (8) as function of the photolysis wavelength is presented in Figure 4. As shown in Figure 4, the relative intensity of the parallel transition has the largest value of about 0.65 at 315 nm, then decreases to about 0.3 at 347 nm and remains almost the

same until 370 nm. It is clear that both the parallel and perpendicular optical transitions contribute to the photodissociation in the spectral region studied. The high values of the relative intensity $\chi_{||}/(\chi_{||}+\chi_{\perp})$ in Figure 4 at short wavelengths indicates the majority of the parallel transition to the $A0^+$ state, while the small value of this intensity at long wavelengths indicates the majority of the perpendicular transitions to the 1(I) and 1(II) states.

The detailed quantitative analysis of the obtained experimental results can be done only by calculation of the excited state population by the photolysis radiation under the conditions of our experiment using ab initio potential energy curves and optical excitation probabilities which have become available now [18], however, some qualitative arguments can be suggested already now. Particularly, as shown in Figure 1, the potential curve of the $A0^+$ state lies higher in energy than the potential curves of the 1(I) and 1(II) states almost in the whole Frank Condon region of the NaI molecule. This fact can explain the majority of the perpendicular transitions in the long-wavelength region from 370 to 347 nm and steep increase of the parallel transition intensity in the shorter wavelengths.

Another argument which can support the experimental result is the kinetic energy dependence of the probability of the nonadiabatic transition between the $A0^+$ and the $X^1\Sigma_0^+$ states at the internuclear distance in the vicinity of 15 a.u. (see Fig. 1). The point is that the depopulation of the $A0^+$ excited state occurs due to the competition between two independent mechanisms: nonadiabatic transition through the potential barrier [16] and radiative decay to the ground molecular state [19]. According to the Landau-Ziner model [26], the nonadiabatic transition probability through the barrier increases exponentially with the fragment recoil velocity (photon energy), while the radiative decay in the first approximation does not depend on the photon energy. Therefore, increasing of the photolysis photon energy increases the quantum yield of the photodissociation reaction via the parallel excitation channel which can result in increasing of β.

As shown by Schäfer et al. [19] and by Baba et al. [21], the absorption spectrum of NaI in the spectral range 300–370 nm contains a large number of well-resolved rotational lines which are grouped with spacing of 36 cm^{-1} and assigned to a vibrational frequency of the $A0^+$ state. The spectrum shows a fragmentary rotational structure having a strong central line with the intensities of the neighboring lines symmetrically decreasing. The majority of the rotational lines are broadened due to the predissociation, the broadening strongly depends on the rotational quantum number with the maximum width up to 370 MHz corresponding to the minimum lifetime of the energy levels of 370 ps [21]. The recorded rotational P and R series showed separation between the neighboring rotational lines of about 4 cm^{-1}.

It should be noted, that the linewidth of the photolysis laser radiation in our experiment was about 0.4 cm^{-1} and therefore the laser line of a particular frequency may fall between the rotational absorption lines of the $A0^+$ state and excite only the two underlying $\Omega = 1$ continua. However, the experimental plot in Figure 4 shows a quite smooth, non-stochastic behavior without steep steps which likely indicates that absorption by the parallel transitions occur at all photolysis wavelengths. This may happen either due to the strong saturation of the individual rotational absorption lines by the pulsed photolysis radiation, or due to the absorption of the very broad quasi-continuum predissociative lines which were not recorded in the high resolution spectroscopy experiments [19,21] because of their small amplitude. Anyway, the above arguments show that the branching ratios of the parallel/perpendicular intensity transitions which are given in Figure 4 are qualitative ones because they likely depend on the overlap between the photolysis laser line and the molecular absorption lines and on the absorption line shapes. Therefore, further clarification of this problem needs additional experiment using a narrow-band photolysis laser whose frequency can be tuned over a molecular rotational line absorption profile. This new experiment is now in preparation in our laboratory.

4 Conclusion

The dependence of the translational anisotropy parameter β on the wavelength of the photolysis light in the photodissociation of NaI in the 315–370 nm spectral range has been studied. The anisotropy parameter β was determined by the analysis of the Doppler absorption profiles of ground state sodium atomic photofragments, recorded at the parallel and perpendicular photolysis light polarization with respect to the direction of the probe laser beam. It was found out that β is always negative in the studied spectral region and decreases monotonely if the photolysis wavelength increases. The obtained β values were used for the analysis of the branching ratio between the intensity of the parallel and perpendicular transitions in NaI photodissociation with particular emphasizing the role of the molecular axis rotation.

The authors are grateful to the Deutsche Forschungsgemeinschaft (contract Zi 186/9-1) and to the Alexander von Humboldt-foundation (contract V-Fokoop) for financial support.

References

1. J.P. Simons, J. Phys. Chem. **88**, 1287 (1984)
2. P.L. Houston, J. Phys. Chem. **91**, 5388 (1987)
3. R.N. Zare, D.R. Herschbach, Proc. IEEE **51**, 173 (1963)
4. L.D.A. Siebbeles, M. Glass-Maujean, O.S. Vasyutinskii, J.A. Beswick, O. Roncero, J. Chem. Phys. **100**, 3610 (1994)
5. V.V. Kuznetsov, O.S. Vasyutinskii, J. Chem. Phys. **123**, 034307 (2005)
6. E.R. Wouters, M. Ahmed, D.S. Peterka, A.S. Bracker, A.G. Suits, O.S. Vasyutinskii, *Imaging the Atomic Orientation and Alignment in Photodissociation, in Imaging in Chemical Dynamics*, edited by A.G. Suits, R.E.

Continetti, ACS Symposium Series (American Chemical Society, Washington DC, 2000)
7. B.V. Picheyev, A.G. Smolin, O.S. Vasyutinskii, J. Phys. Chem. **101**, 7614 (1997)
8. T.P. Rakitzis, R.N. Zare, J. Chem. Phys. **110**, 3341 (1999)
9. P. Davidovits, D.C. Brodhead, J. Chem. Phys. **46**, 2968 (1967)
10. P. Davidovits, D.L. McFadden, *Alkali Halide Vapors* (Academic Press, 1979)
11. T.R. Su, S.J. Riley, J. Chem. Phys. **71**, 3194 (1979)
12. W.R. Anderson, B.M. Wilson, R.C. Ormerod, T.L. Rose, J. Chem. Phys. **74**, 3295 (1981)
13. K.O. Korovin, B.V. Picheyev, O.S. Vasyutinskii, H. Valipour, D. Zimmermann, J. Chem. Phys. **112**, 2059 (2000)
14. K.O. Korovin, A.A. Veselov, O.S. Vasyutinskii, D. Zimmermann, Opt. Spectrosc. **93**, 530 (2002)
15. K.O. Korovin, A.A. Veselov, E.M. Mikheev, O.S. Vasyutinskii, D. Zimmermann, Opt. Spectrosc. **99**, 880 (2005)
16. P. Cong, A. Mokhtari, A.H. Zewail, Chem. Phys. Lett. **172**, 109 (1990)
17. J.L.Herek, A. Materny, A.H. Zewail, Chem. Phys. Lett. **228**, 15 (1994)
18. A.B. Alekseyev, H.-P. Liebermann, R.J. Buenker, N. Balakrishnan, H.R. Sadeghpour, S.T. Cornett, M.J. Cavagnero, J. Chem. Phys. **113**, 1514 (2000)
19. S.H. Schäfer, D. Bender, E. Tiemann, Chem. Phys. **89**, 65 (1984)
20. H. Bluhm, J. Lindner, E. Tiemann, J. Chem. Phys. **93**, 4556 (1990)
21. M. Baba, T. Kokita, S. Kagahara, H. Kato, J. Chem. Phys. **111**, 9574 (1999)
22. G. Herzberg, *Molecular Spectra and Molecular Structure I. Spectra of Diatomic Molecules* (Van Nostrand Reinhold, New York, 1950)
23. C. Jonah, J. Chem. Phys. **55**, 1915 (1971)
24. R. Liyanage, R.J. Gordon, J. Chem. Phys. **107**, 7209 (1997)
25. V.V. Kuznetsov, O.S. Vasyutinskii, J. Chem. Phys. (to be published, 2007)
26. E.E. Nikitin, S.Ya. Umanskii, *Theory of Slow Atomic Collisions* (Springer, Berlin, 1984)